3rd Middle East Turbomachinery Symposium (METS III)
15-18 February 2015 | Doha, Qatar | mets.tamu.edu

STALL INDUCED AERODYNAMIC FORCING AND ROTOR VIBRATIONS IN A MULTISTAGE CENTRIFUGAL COMPRESSOR

Dr. Davide Biliotti
Lead Engineer
GE Oil & Gas – Nuovo Pignone
Florence, Italy

Dr. Elisabetta Belardini
Senior Engineer
GE Oil & Gas – Nuovo Pignone
Florence, Italy

Dr. Marco Giachi
Principal Engineer
GE Oil & Gas – Nuovo Pignone
Florence, Italy

Dr. Lorenzo Toni
Lead Engineer
GE Oil & Gas – Nuovo Pignone
Florence, Italy

Dr. Giuseppe Vannini
Principal Engineer
GE Oil & Gas – Nuovo Pignone
Florence, Italy

Dr. Dante Tommaso Rubino
Engineering Manager
GE Oil & Gas – Nuovo Pignone
Florence, Italy

Davide Biliotti received the degree in Mechanical Engineering at the Department of Industrial Engineering of the University of Florence (Italy) in 2010. In the December 2013 he completed his doctorate in Energy and Innovative Industrial and Environmental Technology. His PhD project, conducted in collaboration with GE Oil & Gas, was based on the analysis of the rotating stall phenomenon in centrifugal compressors by means of experimental and numerical approaches. Now, he is working as Aerodynamic Design Engineer in the Advanced Technology Organization in GE Oil & Gas.

Lorenzo Toni is a Lead Engineer in the Radial Turbomachinery Aerodynamic Design Team within the Advanced Technology organization of GE Oil & Gas. Lorenzo joined GE in 2009 as a Test and Acquisition Engineer and then moved in the present position. He received an M.S. degree in Mechanical Engineering from the Florence University in 2005 and earned a PhD in Energetics from the same University in 2009, with a doctoral thesis on "Gas Turbine Aero-Engines Effusion Cooling Systems". He is the author or co-author of several technical papers in the field of turbomachinery.

Elisabetta Belardini is Senior Engineer of Radial Turbo machinery Performance within the Advanced Technology Division of GE Oil & Gas Company, in Florence, Italy. Her responsibilities include performance predictability and risk assessment of the GE Oil & Gas compressors, stall investigation and modeling of system dynamics. Elisabetta joined GE in 2005 as Test Engineer and then moved in present role in the Advanced Technology team. Elisabetta received a M.S. degree with honor in Mechanical Engineering in 1996 and a Ph.D. in Energetics in 2000 from University of Florence followed by a four year post-doctoral research in the unsteady CFD simulation of turbo machinery rows. She has authored or coauthored technical papers, in the area of CFD, stall modeling and compressor performance

Giuseppe Vannini is a Principal Engineer in the Advanced Technology Organization of GE Oil & Gas, which he joined in early 2001. He has been involved in advanced rotordynamic studies on high performance centrifugal compressors developing both analytical and experimental research activities. After leading the first subsea compressor prototype design up to the final FAT he came back to full-time rotordynamic activity and he's active especially in the field of annular seals modeling and testing, advanced gas and oil bearings validation. He holds a PhD in Mechanical Engineering at Pisa University and he's member of API684 Task Force.

Marco Giachi is a Principal Engineer in the Aero Team of the Advanced Technology Organization of GE Oil & Gas. Marco received a M.S. degree with honor in Aerospace Engineering at Pisa University in 1985 and he graduated with honors in the Diploma Course program at the von Karman Institute in 1987. Marco joined GE in 1994 after some years spent in aerospace and automotive industries. Since then he has been involved in design, RCA and development of centrifugal compressors components. He is the author or co-author of

several technical papers in the field of turbomachinery and manuals

Tommaso Rubino is currently the Manager of the Radial Turbomachinery Aerodynamic Design and Performance within the Advanced Technology Division of GE Oil & Gas Company, in Florence, Italy. His responsibilities include the aerodynamic design and the performance predictability of the GE Oil & Gas turbocompressors and turboexpanders product lines. Dr. Rubino joined GE in 2006 as Design Engineer in Centrifugal Compressor NPI team, then rolling in the Aero team upon creation of the Advanced Technology Organization, where he has been responsible of the aerodynamic design of new stage families for Centrifugal Compressors. Mr. Rubino received an M.S. degree in Mechanical Engineering in 2002 and a Ph.D. degree in Mechanical Engineering in 2006 from Politecnico of Bari, and he graduated with honors in the Diploma Course program at the von Karman Institute in 2002.

ABSTRACT

The Oil & Gas industry is looking with increased interest at solutions for improving operating flexibility of centrifugal compressors. The stable operation of a compressor stage or machine is generally limited at the left of operating range by the occurrence of a local aerodynamic unsteady phenomenon, the rotating stall, which usually precedes the surge. Rotating stall could cause, depending on the actual operating conditions, severe sub-synchronous vibrations to the rotor which may compromise rotordynamic behavior, preventing the machine from operating at very low flow rates. An accurate characterization of rotating stall phenomena, and their impact on rotordynamic stability, may represent an important step forward in centrifugal compressor design and performance predictability, insofar as it allows to correctly predict the real operating range of the machine.

In recently published works the authors presented a procedure which allows reconstructing the pressure unbalance due to the diffuser rotating stall, to estimate the rotating force acting on the shaft and, by means of a rotordynamic model, the vibration at the bearings. In addition to this, a criterion to scale the rotating force coming from model test conditions up to full-scale machine conditions has been developed and successfully validated.

In this framework a thorough work has been performed to apply the aforementioned procedure to an LNG multistage compressor.

Firstly, the stages which equip the machine were tested as single scaled-down stages in a model test rig, in order to fully characterize their dynamic behavior while approaching the left limit and operating in stall condition. Then, the full scale machine has been equipped with dynamic pressure probes in different locations along the gas flow path, and has been tested according to ASME PTC-10 standard; this allowed to capture the stall inception and its evolution and finally to get the rotating pressure pattern acting on the rotor. A noticeable agreement was obtained between the force resulting from the pressure field integration and the one obtained through a proper scaling of the test data.

Finally, the calculated stall force has been used as an input in a rotordynamic model of the whole compressor: the predicted Subsynchronous Vibration (SSV) estimated at the displacement probe location has been compared with the measured value showing some differences which can be related to the proximity of the first rotor mode.

INTRODUCTION

In current industrial compressor field, increasing efforts are devoted to explore new aerodynamic solution both to maximize the efficiency and to extend the limits of the operating curve in order to improve the operating flexibility of the machine.

Within this scenario, great interest has been paid by the research on analyzing the unsteady phenomena that precede the surge and determine the left limit of the curve.

In particular, rotating stall represents one of the main unsteady phenomena which not only influence the performance of the compressor, but also can generate severe subsynchronous vibrations to the rotor avoiding the machine to operate beyond this limit.

With this in mind, it is worth to note that an accurate characterization of rotating stall could play a key role in the centrifugal compressor design. To do so, a systematic approach based on the manipulation of the experimental data coming from dynamic pressure probes flush mounted inside the flow path has been recently developed and validated by authors Bianchini et al. (2013) (2014) and Biliotti et al (2014). Thanks to this procedure it was possible both to reconstruct the pressure unbalance at a certain section during stall condition and to estimate the rotating force acting on the rotor shaft.

As a first step, in order to investigate the rotordynamic behavior of the machine during stall condition, some the stages of the multistage compressor have been tested as single scale-down stages in a model test rig. Then, also the whole compressor was equipped with dynamic pressure probes and tested according to ASME PTC-10 standard.

Once the rotating stall has been characterized, a validated criterion developed by the authors has been applied to scale the force value from the model test condition to the full scale multistage compressor condition.

By doing so, the aerodynamic stall force calculated by means of dynamic pressure probes, installed in a model test, has been first compared with that one obtained in the whole compressor and then verified with a specific rotordynamic code used to predict the rotordynamic behavior.

EXPERIMENTAL CAMPAIGN – MODEL TEST

Test Rig Layout and Instrumentation

A twofold experimental campaign has been carried out for the purposes of the present work: model testing activity was indeed required to obtain the stall related forces which had to be scaled, through a proper correlation, and compared to the full scale machine ones.

As already mentioned, the stages which equip the multistage machine have been at first model tested.

Model testing activity was carried out at the GE Oil & Gas Technology Laboratory (OGTL) in Florence. The test bench

consisted of a closed loop rotating single stage rig, normally employed for performance measurements of different centrifugal compressor designs; further details can be found Toni et al. (2010), Bianchini et al. (2013) and in Guidotti et al. (2011). The compressor was driven by a 3 MW electric motor that was connected to the shaft through a fluid drive and a gear box and throttled by means of two ball valves.

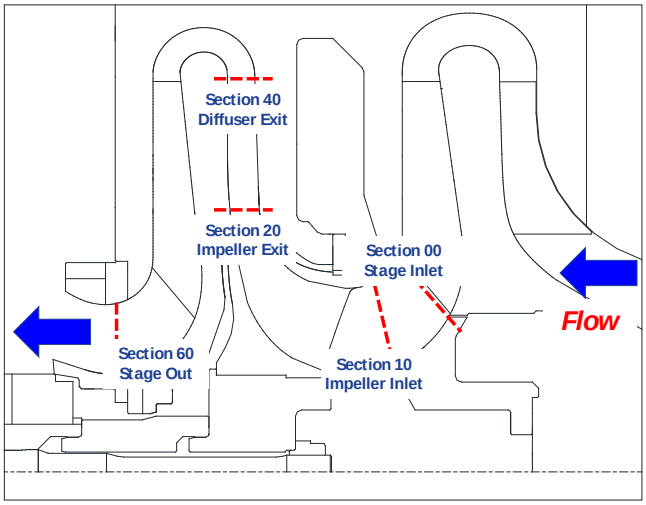

Figure 1 - Schematic Cross Section of a Model Test Stage

All the results presented in this paper, as far as model tests are considered, are obtained from experiments using R134a as working gas (molecular weight = 102 kg/kmol) and an average suction pressure of around 1.1 bar.

The tested stages included an inlet plenum (or upstream return channel, depending on the particular stage considered), the impeller, a vaneless diffuser and a return channel (or discharge scroll), see Figure 1.

According to such scheme, the main measurements sections are indicated as:

- Section 00: Stage Inlet
- Section 10: Impeller Inlet
- Section 20: Impeller Outlet / Diffuser Inlet
- Section 40: Diffuser Outlet / Return Channel Inlet
- Section 60: Stage Outlet / Return Channel Outlet

The test rig was instrumented with total temperature and total pressure rakes to allow flange-to flange measurements. Measurements were also taken at various locations throughout the test article to derive single component (i.e. impeller, diffuser, return channel, …) performance. The measurements of total pressure were performed with Kiel probes, total temperature with shielded J-type thermocouples and flow angles with three-hole and five-hole probes. At each of the measurement locations throughout the compressor, static pressure taps were positioned around the circumference of both the hub and the shroud sides. At the impeller inlet (Section 10), the probes were assembled as rakes and were mounted on a rotating conveyor which enabled the acquisition of high resolution measurements. The mass flow was measured with an orifice flow meter that uses a combination of differential pressure and temperature measurement, according to EN ISO 5167 standard; whereas the rig rotating speed was measured using a magnetic pick-up based key-phasor. The rotor vibrations have been acquired at three locations along the shaft length. Both on the DE an NDE side of the compressor, the vertical and horizontal vibrations were monitored with eddy current proximity probes. The axial vibration was measured using an eddy current probe as well. Steady state controls for point acquisition were performed both on flow coefficient and peripheral Mach number, as well as on rig thermal stability and stage performance: as a general rule the controls which are set in the acquisition software algorithm are about an order of magnitude stricter than the ASME PTC10 ones.

Dynamic pressure measurements were carried out in various location of the stage. High-sensitivity piezoelectric sensors, manufactured by PCB, having a resonance frequency over 250 kHz, were installed at sections 10, 20 and 40. In the diffuser sections (20 and 40) 3 probes are installed at the same radius and at different tangential positions, in order to determine phase shift which will be required in data processing. Table 1 summarizes the dynamic sensors installed in the various sections of the stage.

All the dynamic signals have been continuously recorded with a bandwidth of 20 kHz. Both real-time and off-line analyses have been performed by means of GE proprietary softwares.

Section	Sensor Type	Number of Sensors
10	PCB 102M206	1
20	PCB 102M206	3
40	PCB 102M206	3

Table 1 – Dynamic Pressure Measurements

Model Test Results

For sake of simplicity, only the results related to the second stage, which was the most critical in term of rotating stall (i.e. the first one to reach the stall condition), will be reported in this section.

Stall analysis is experimentally carried out by reducing compressor flow rate from choke condition up to surge occurrence: unsteady pressure signals, as well as shaft vibrations, are analyzed and stall inception is identified by the rising up of sub-synchronous phenomena. Once stall region is identified, a detailed analysis of rotating stall is then performed.

As a first step, the power spectrum of each dynamic pressure sensors was monitored during the stall occurrence in order both to highlight the characteristic frequencies and to verify the agreement between the sensors themselves in term of measured amplitude. Figure 2 shows the power spectrum of one of the PCB located at section 20 presented in a dimensionless form (i.e. the amplitude is divided by the maximum value (A*) and the frequency is divided by the rotation frequency of the impeller). Three main contributions are clearly distinguishable: the subsynchronous one corresponds to the stall frequency, while the others are the stall second harmonic and the Blade Passing Frequency (BPF) respectively.

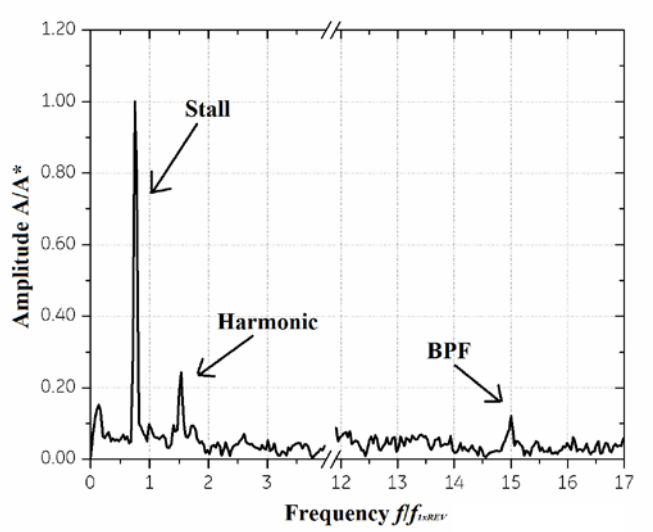

Figure 2 - Power Spectrum of a Pressure Probe at Section 20

After these preliminary checks, a correct estimation of the period of the phenomenon was needed in order to perform a correct averaging process (i.e. to average the time data really connected to the same interval).

In order to determine the stall frequency and consequently pressure distribution with more accuracy than the previous time-frequency analysis presented, as a second step of the developed procedure, the auto-correlation and cross-correlation functions were applied. By means of these functions, which relate time signals of a sensor both with itself and with the others at the same section, it is possible to identify with a higher accuracy both stall frequency and phase shift, thus leading to determine the lobes' number. For further details on this approach, please refer to Bianchini et al. (2013).

As reported in Ferrara et al. (2004), once the frequency of the phenomenon has been identified, before to proceed with the ensemble average, clocked on the stall frequency, some important assumptions must be done:

- The stall pattern is supposed to rotate as a rigid body at a certain subsynchronous frequency.
- The stall pattern is supposed to be uniform between the hub and the shroud.

In order to perform the ensemble average approach of the time signal in a specific interval, the previous assumptions must be satisfied; if the frequency of the rotating stall has been correctly detected, the averaging process provides the average quantity of that specific period.

By exploiting the hypothesis on the rigid body rotation, is now possible to relate the time domain to the spatial domain; in other words, one can correlate the time interval in which the averaging process has been performed to a spatial angular sector.

As a result, the pressure pattern after the ensemble average process is shown in Figure 3. One can readily notice that the analysis pointed out the single lobe nature of this stall, in which the pressure unbalance rotates at a frequency of 74% of the rotational frequency (f_{1xREV}) inside the diffuser.

The lobes' number is given by the ratio between the phase shift ($\Delta\vartheta$) and the geometrical shift ($\Delta\alpha$) and it can be easily calculated with Eq. (1):

$$N = \left.\frac{\Delta\vartheta}{\Delta\alpha}\right|_{f=f_l} \qquad (1)$$

where the subscript l indicates the frequency of the lobe passage that in case of a single lobe corresponds to the stall frequency.

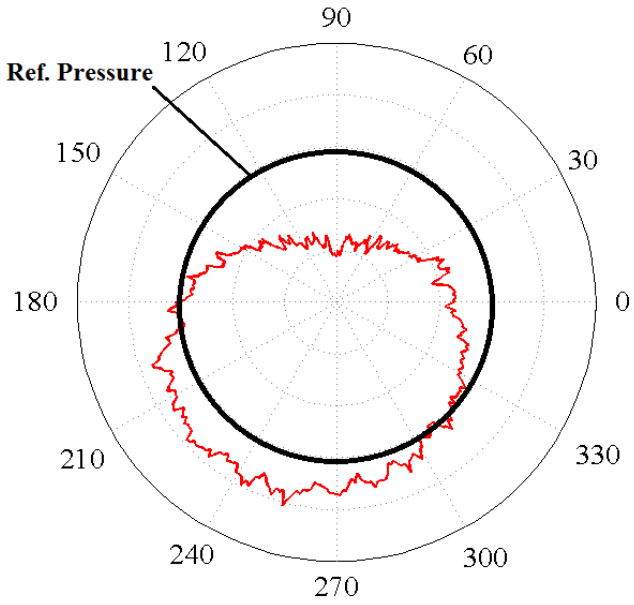

Figure 3 – Polar distribution of the single-lobe stall pattern measured on the model test at Section 20

EXPERIMENTAL CAMPAIGN – FULL SCALE COMPRESSOR

Test Rig Layout and Instrumentation

The full-scale multistage compressor, equipped with the three stages whose scaled down version was model tested, has been tested in a dedicated facility located in Massa plant, where a type-2 performance test, as specified in ASME PTC-10 standard, was carried out.

Besides the instrumentation prescribed by this standard, test rig was equipped with dynamic pressure probes (piezoelectric sensors, manufactured by PCB), that were installed in various locations of the gas path, as sketched in Figure 4 and listed in Table 2. Since model tests revealed rotating stall occurrence for the second stage, 4 dynamic pressure sensors (at the same radius and with a geometrical shift equal to 180°) have been placed downstream of such stage so as to correctly reconstruct the stall related rotating pressure pattern. As far as vibrations are concerned, eddy current proximity probes have been used on both DE and NDE sides.

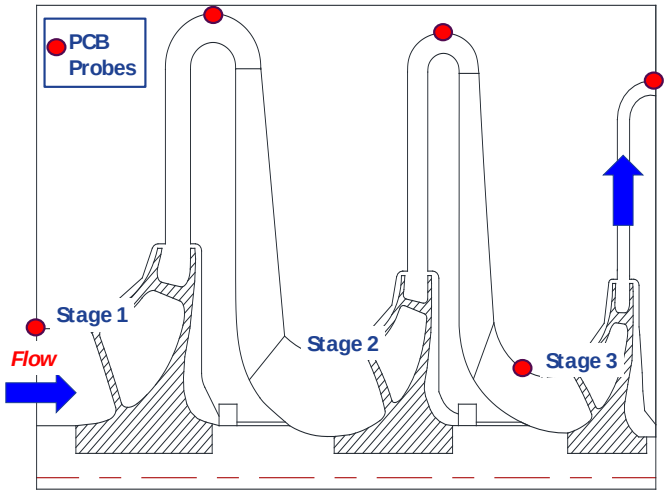

Figure 4 - Schematic of the Instrumentation Installed on the Multistage Full Scale Compressor

Section	Sensor Type	Number of Sensors
Inlet Volute	PCB 102M206	1
Stage 1 Exit	PCB 102M206	1
Stage 2 Exit	PCB 102M206	4
Stage 3 Inlet	PCB 102M206	1
Discharge Scroll	PCB 102M206	1

Table 2 – Dynamic Pressure Measurements

Full Scale Test Results

In order to investigate the rotordynamic behavior during stall conditions, the same procedure, used for the model test, was applied to the experimental data reordered by PCBs properly distributed along the flow path (see Figure 4).

In particular, as expected, sensors positioned at the exit of Stage 2 highlight the highest oscillation in term of pressure unbalance. In Figure 5 is reported the power spectrum obtained from one of these 4 PCBs presented again in a dimensionless form (i.e. the amplitude is divided by the maximum value (A*) and the frequency is divided by the rotation frequency of the impeller).

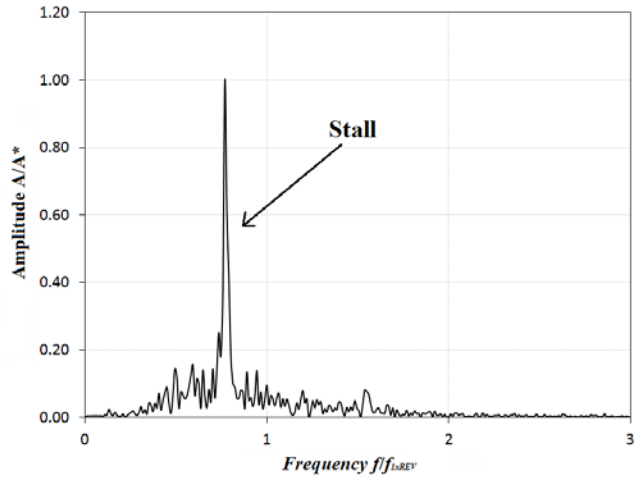

Figure 5 – Power Spectrum of a Pressure Probe at Stage 2 Exit

It is worth to note that in this case the subsynchronous peak represents the main contribution in the frequency domain and neither rotational frequency nor harmonics are distinguishable. The stall frequency of 77% of the rotational frequency (f_{1xREV}) was estimated by means of the systematic procedure presented before; one can easily notice that a very good agreement between the frequency measured in the whole compressor and that one obtained in the relative model test was obtained.

The pressure pattern reconstruction showed, again, a single lobe stall. Moreover, as a further confirmation, in Figure 6, two dynamic pressure signals cut in a time window corresponding to the stall frequency are presented.

According to Bianchini et al. (2014) the number of lobes is also confirmed by the phase shift of 180° between the two PCBs calculated by means of a cross correlation function.

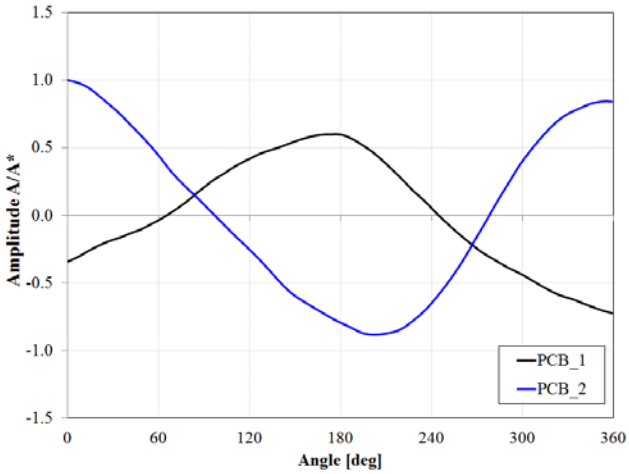

Figure 6 – Two PCBs Signals at Stage 2 Exit Plotted in the Space Domain

ROTATING STALL FORCE CALCULATION AND SCALING CRITERION

The last step of the analysis was to estimate a rotating stall force acting to the rotor shaft and to correlate it with the rotordynamic behavior of the machine.

Once the stall pattern has been reconstructed both for the model test and the whole compressor, the unbalancing force acting radially to the rotor is indeed given by Eq. (2), i.e. considering the resultant of the non-axisymmetric pressure pattern around the impeller and integrating the pressure on the area on which it is measured.

$$F_{stall} = \int_0^{2\pi} p(\alpha) b_{sect} R_{sect} d\alpha \qquad (2)$$

In order both to show the results and to compare the two cases with different geometric characteristics and design points, a dimensionless coefficient already defined and verified by the authors was used, as in Eq. (3).

$$\chi = \frac{F_{stall}}{0.5 \cdot \rho_2 \cdot c_2^2 \cdot S_2} \qquad (3)$$

The χ coefficient allowed correlating the stall force with the dynamic pressure and the geometrical characteristics at the exit of the impeller. By applying this formulation both to the model test and the whole compressor, a value of about 0.02 was obtained Table 3; the good agreement between the two values confirms that the χ coefficient can be used to scale the force value obtained in a model test to a multistage compressor (if constituted by impellers coming from the same family) operating in different conditions.

	Model Test	F. S. Compressor
χ	0.018	0.021
f/f_{1xRev}	74%	77%

Table 3 – Non-Dimensional Force Coefficient

ROTORDYNAMIC MODEL: ASSUMPTIONS AND RESULTS

Assumptions

The rotordynamic model of the compressor was assessed by an available numerical code based on a finite elements approach. The schematization used in the code is reported in Figure 7, coupled with the mechanical drawing of the rotor.

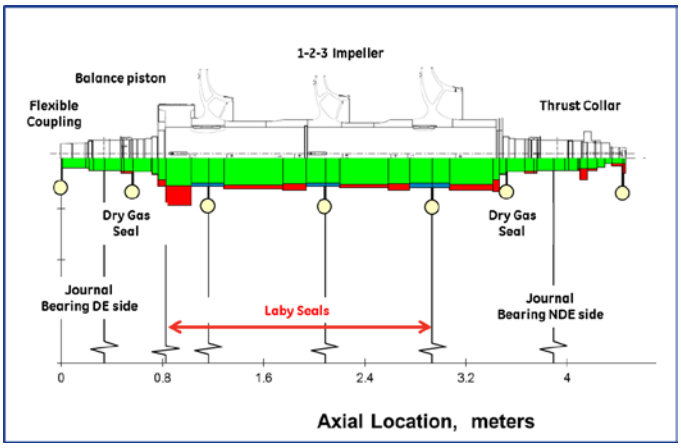

Figure 7 - Rotordynamic Model of the Compressor.

Upon examination of the figure, the main rotor features can be readily noticed:

- "Beam Rotor" design: the rotor is typical of a multistage compressor where the impellers are located between the journal bearings;

Furthermore, all the elements green in color have both stiffness and inertial properties while the red in color elements have inertial properties only;

- Each impeller is modeled as a lumped inertia (the relevant mass and polar/transverse inertia are placed in the center of gravity).
- Among the other main items: the flexible coupling presence at the drive end side is modeled through a lumped mass placed in the relevant center of gravity (as well as the Dry Gas Seals). On the contrary the thrust collar and the balance piston are modeled through real geometry as inertial elements.
- Journal bearings locations are also indicated. They are hydrodynamic tilting pad type bearings and they are modeled through a pair of stiffness and damping matrices. Synchronous reduced coefficients are computed through a numerical code capable of accounting for pad pivot flexibility and pad thermal-mechanical deformations Branagan et al. Synchronous reduced coefficients are used here following both the design standard guidelines [API 617] and Company authors' internal practice.
- Internal seals locations are also identified. The seals effects can be accounted for through the relevant dynamic coefficients. For this specific compressor only labyrinth seals are adopted (tooth on stator on impeller eyes and tooth on rotor on balance piston). The laby seal code which is used at Authors' Company is described by Thorat et al. (2009).

Usually the seal coefficients are accounted for in the stability analysis only, since the overall rotor damping factor is of primary interest in this analysis and the seals have a major impact on the rotor effective damping (due to their high cross coupled stiffness term, see Eq. 4). For this specific forced response analysis (performed at full load condition), they theoretically may have an impact as well. From a practical viewpoint, if only labyrinth seals are present, the forced response is almost unaffected in the low frequency region (i.e. far from the rotor natural frequency) because the seals contribution to the effective stiffness (see Eq. 5) is negligible with respect to the journal bearings contribution. At very low frequency in fact the rotor system behaves like a mass-spring system (see Figure 8 which is extracted from Biliotti et al. (2014).

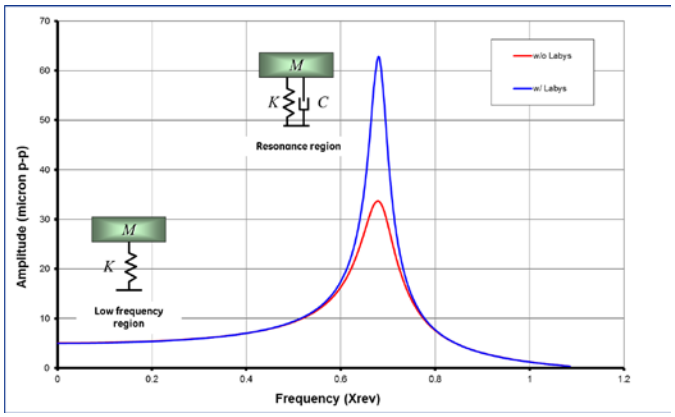

Figure 8 – Labyrinth Seal Effect on Rotor Damped Forced Response.

On the other hand, in the frequency range near the natural frequency (where the effective damping is more important), they can effectively reduce the system damping (the rotor behaves like a mass-spring-dashpot system). Anyway for this specific case, since the pressure level is quite low (discharge pressure is below 15 bara) even the impact on the effective damping is low (as shown later in the results paragraph).

$$C_{eff} = C_{xx} - K_{xy}/\omega \quad (4)$$

$$K_{eff} = K_{xx} + C_{xy} \cdot \omega \quad (5)$$

The calculated aerodynamic force in each load case was

finally applied to the rotordynamic model in the location of the critical impeller center of gravity (e.g. the force is applied only on the impeller relevant to the stage which is more likely to exhibit a rotating stall).

The forced response to the aerodynamic excitation was modeled via the asynchronous response module of the software which is able to predict the behavior of the rotor subject to an external load which is not synchronized with the running speed (differently from the more conventional study case of rotor imbalance). In details, the external excitation was modeled as a rotating force with constant amplitude (scaled through Eq. (3)) and variable frequency.

The whole subsynchronous range was investigated, although special attention was reserved to the range around 77% of f_{1xREV} that was experienced in the test as rotating stall frequency.

Results

Based upon the rotordynamic model defined above the forced response to the rotating stall force was computed. Figure 9 is showing the predicted vibration amplitudes compared with the measured vibration at the frequency in object, namely 0.77 f_{1xREV}. The predicted values are roughly lower by a factor 1.5. This is a worse outcome with respect to the previous results showed by Bianchini et al. (2013) which showed an agreement within few percent. According to the Authors' opinion, the likely reason for the higher discrepancy is the close proximity of the rotating stall frequency to the first rotor mode (which is predicted and measured at 0.88 f_{1xREV}) for this specific case. This makes more difficult the comparison because the vibration level induced by the aerodynamic force is also affected by the rotor first resonance (like a superimposition of the two effects).

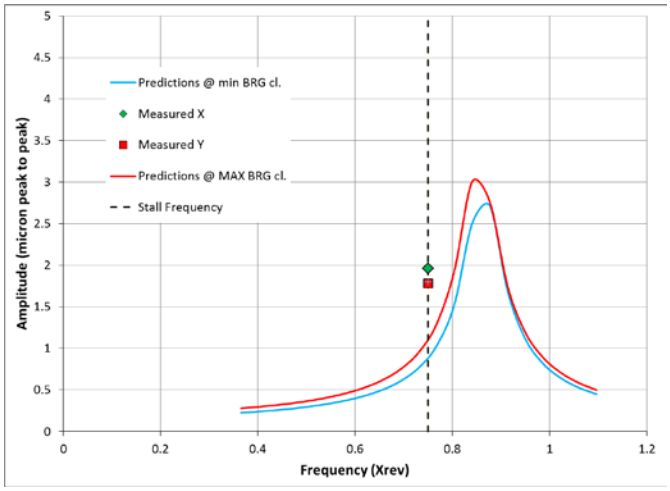

Figure 9 – Predicted vs. Measured Vibration Amplitude.

It is worth to say the prediction of the first rotor resonance is in reasonable agreement with the experimental data and it is also clearly possible to distinguish the two different vibration phenomena (the rotating stall induced vibration and the first rotor natural frequency). This is shown by the following waterfall plot in Figure 10 where vibrations are showed both during the stall event and the following run-down. During the stall event is clear to see the concurrent presence of both vibration phenomena: the 0.77 f_{1xREV} which is related to the rotating stall (reaching few microns amplitude) and the 0.88 f_{1xREV} which is the first natural frequency (being lower than 1 micron and visible just due to the high spectral resolution). During the run-down is anyway possible to confirm that the 0.88 f_{1xREV} frequency is the rotor first natural frequency since there is the critical speed resonance region around.

The present results confirm the general validity of the vibration predictive method due to the reasons stated above.

Moreover, it is noteworthy that the amplitude of stall related vibrations is well below the acceptance criterion as per API 617 standard.

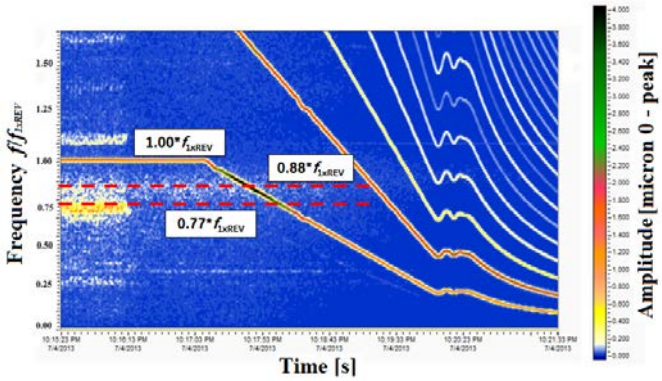

Figure 10 – Waterfall Plot Showing Stall Event & Run-Down.

CONCLUSIONS

In this work a validated procedure to evaluate the effects of a rotating stall on the aerodynamic behavior of a centrifugal compressor has been applied both to an LNG multistage compressor and to the relative single scaled-down stages. If on one hand, dynamic pressure measurements are commonly used in a single scaled-down stage, on the other hand in this activity also the full multistage compressor was equipped with several PCBs positioned at the outer radius of the flow-path.

Thanks to this proper instrumentation, the procedure allowed to reconstruct the pressure pattern during stall conditions inside the diffuser of the second stage which was deemed to be the most critical (i.e. the first one to reach the stall condition) and to verify the agreement between the force resulting from the pressure field integration and the one obtained through a proper scaling criterion starting from the single stage test.

The analysis of the data coming from dynamic pressure probes installed both in the single model test and in the multistage compressor showed a very good agreement in terms of the stall frequency (0.74 f_{1xREV} and 0.77 f_{1xREV}, respectively) and the rotating force (χ 0.018 and χ 0.021, respectively).

Once the experimental agreement was verified, a rotordynamic model of the whole compressor was developed in order to evaluate the prediction capability of the machine behavior during the stall by comparing the measured vibration with the predicted one. As in the previous authors' works, the relation between stall and rotordynamic vibration is definitely confirmed also by this approach even if with a higher difference, likely due to the proximity of the rotating stall frequency to the first rotor mode.

The first attempt to transfer the aerodynamic stall force calculated by means of dynamic pressure measurements carried out at the model test rig into a predicted vibration of the whole compressor operating in on-site conditions was presented by Bianchini et al. (2013). This work represents a further step in the direction of building a strategy to extend model test results to full scale machine, with the final aim of extending the left margin of the performance curves based on the model results.

NOMENCLATURE

b	Diffuser width	*[m]*
p	Pressure	*[Pa]*
c	Absolute velocity	*[m/s]*
C_{eff}	Effective damping	*[Ns/m]*
C_{ij}	Direct/cross coupled damping coeff.	*[Ns/m]*
K_{eff}	Effective stiffness	*[N/m]*
K_{ij}	Direct/cross coupled stiffness coeff.	*[N/m]*
A	Amplitude	*[mbar; µm]*
S	Area	*[m^2]*
R	Radius	*[m^2]*
F	Stall force	*[N]*
f	Frequency	*[Hz]*
N	Number of lobes	*[-]*
FFT	Fast Fourier Transform	*[-]*
BPF	Blade Passing Frequency	*[-]*

Greeks

α	Azimuthal angle	*[deg]*
$\Delta\alpha$	Angular shift between two sensors	*[deg]*
$\Delta\vartheta$	Phase shift between two sensors	*[Hz]*
ρ	Gas density	*[kg/m^3]*
χ	Dimensionless force coefficient	*[-]*

Greeks

1xREV	Rotational frequency
2	Outlet section of the impeller
sect	Analyzed section
l	Lobe

ACKNOWLEDGEMENTS

The authors would like to express their gratitude to GE Oil & Gas for the permissions to proceed with publication. Thanks are due to the Design Engineer of the compressor Mirto Tondini for his support during the field testing and Prof. Giovanni Ferrara, Dr. Lorenzo Ferrari and Dr. Alessandro Bianchini from University of Florence.

REFERENCES

Bianchini, A., Biliotti, D., Ferrara, G., Ferrari, L., Belardini, E., Giachi, M., Tapinassi, L. and Vannini, G., 2013, "A systematic approach to estimate the impact of the aerodynamic force induced by rotating stall in a vaneless diffuser on the rotordynamic behavior of centrifugal compressors," *Journal of Engineering for Gas Turbines and Power,* 135(11), pp. 1-9.

Bianchini, A., Biliotti, D., Ferrara, G., Ferrari, L., Belardini, E., Giachi, M. and Tapinassi, L., 2014, "Some guidelines for the experimental characterization of vaneless diffuser rotating stall in stages of industrial centrifugal compressors," Paper published in *Proc. of the ASME Turbo Expo 2014, Düsseldorf, Germany*, June 16-20, 2014.

Biliotti, D., Bianchini, A., Ferrara, G., Ferrari, L., Belardini, E., Giachi, M., Tapinassi, L. and Vannini, G., 2014, "Analysis of the rotordynamic response of a centrifugal compressor subject to aerodynamic loads due to rotating stall," Paper published in *Proc. of the ASME Turbo Expo 2014, Düsseldorf, Germany*, June 16-20, 2014.

Toni, L., Ballarini, V., Cioncolini, S., Persico, G. and Gaetani, P., 2010, "Unsteady flow field measurements in an industrial centrifugal compressor", *39th Turbomachinery Symposium*, pp 49-58.

Bianchini, A., Ferrara, G., Ferrari, L., Ballarini, V., Bianchi, L., Tapinassi, L. and Toni, L., 2012, "Effects due to the Temperature Measurement Section on the Performance Estimation of a Centrifugal Compressor Stage", *Journal of Engineering for Gas Turbines and Power*, 134, pp. 1-9.

Guidotti, E., Tapinassi, L., Toni, L., Bianchi, L., Gaetani, P. and Persico, G., 2011, "Experimental and numerical analysis of the flow field in the impeller of a centrifugal compressor stage at design point", *ASME Paper 2011-45036.*

Ferrara, G., Ferrari, L. and Baldassarre, L., "Rotating Stall in Centrifugal Compressor Vaneless Diffuser: Experimental Analysis of Geometrical Parameters Influence on Phenomenon Evolution," *Journal of Rotating Machinery*, n. 10(6), pp. 433-442, 2004.

J. Colding-Jørgensen, "Effect of fluid forces on rotor stability of centrifugal compressors and pumps," NASA, Lewis Res. Center Rotordyn, 1980.

J. Colding-Jørgensen, "Prevention of Rotordynamic Problems in High Pressure Centrifugal Compressors," in *Proc. of the 1st International Conference on Turbomachinery, Rotating Equipment and Condition Monitoring Equipment*, Singapore, July 20-22, 1994.

Ishimoto, L., Silva, R. T., Rangel, J. S., Jr., Miranda, M. A., Audehove, F. N., Marques, B. S., Baldassarre, L. and Paut, C., "Early detection of rotating stall phenomenon in centrifugal compressors by means of ASME PTC 10 type 2 test," in *Proc. of the Forty-First Turbomachinery Symposium*, Houston, Texas, USA, September 24-27, 2012.

Turbomachinery Research Consortium, 2002, "XLTRC2 Rotordynamics Software Suite (2002)", *Turbomachinery Laboratory, Texas A&M University, Tech. Rep*.

Branagan, L. and Barrett, L., "Annex 4 – Tilting pad Dynamic

Coefficient Reduction with pivot flexibility" *UVA Report No. UVA/643092/MAE88/376*.

Thorat, M. and Childs, D.W., 2009, "Predicted rotordynamic behavior of a labyrinth seal as rotor surface velocity approaches Mach 1," *Proceedings of ASME Turbo Expo 2009, Orlando, USA*, June 8-12, 2009.

Kleynhans, G. and Childs, D.W., 1997, "The acoustic influence of cell depth on the rotordynamic characteristics of smooth-rotor/honeycomb-stator annular gas seals," *Journal of Engineering for Gas Turbine and Power*, 119, pp. 949-957.

API, 2002, "Axial and Centrifugal Compressors and Expander-compressors for Petroleum, Chemical and Gas Service Industry," *API Standard 617, 7th Edition*.